Non-hydrostatic modelling at the Met Office

Terry Davies

Met Office, University of Reading, Reading
RG6 6BB, United Kingdom
terry.davies@metoffice.gov.uk

1 Introduction

The first Met Office non-hydrostatic model was developed by Tapp and White (1976). Height-based terrain-following coordinates were introduced by Carpenter (1979) and physical parametrizations by Golding (1987). It was used for process studies (Ballard et al., 1991) and from 1988 ran operationally but was its usefulness was limited by its coarse (15km) horizontal resolution and its lack of a state-of-the-art data assimilation system. Golding (1992) upgraded the model to use a 2 time-level (2TL) semi-Lagrangian scheme (Temperton and Staniforth, 1987 McDonald and Bates, 1987) but overall this had little impact on the model efficiency since the use of larger time steps was limited by lateral boundary errors.

In the 1992 development of this non-hydrostatic model was stopped and the first (hydrostatic) Unified Model (UM, Cullen and Davies, 1991) was used to run what was called the Mesoscale Model configuration at 16km resolution. The UM was developed to be used for all production models in NWP and climate and its main requirement, in addition to being efficient, was to (formally) conserve mass in long (centuries) climate runs. It was also decided to use the deep atmosphere equations (White and Bromley, 1995) to reduce approximation to the full equations. The UM used a split-explicit scheme similar to that used in operational NWP at the Met Office since the mid-1970's (Gadd, 1978).

In the early 1990's development of the non-hydrostatic New Dynamics (ND) began and it was already clear that there were advantages to be gained in using both a semi-implicit time scheme and semi-Lagrangian advection (SISL, Staniforth and Côté, 1991). An overview of the proposed ND design together with some idealised tests was presented by Mike Cullen at the André Robert Memorial Symposium in 1994 (Cullen et al., 1997). An outline of the ND together with results from idealised tests and short climate tests appear in (Davies et al., 1998). The details of the discretization and method of solution can be in Davies et al. (2005). A comprehensive description is presented in Staniforth et al. (2006).

The non-hydrostatic UM, together with new versions of the physics parametrizations (Martin et al., 2006) began operations in the summer of 2002. The UK mesoscale resolution had a horizontal resolution of 12km and testing of 1km and 4km versions began soon after. A 4km version of the UM began routine running in 2005 (largely as a result of the Boscastle storm which also led to the option to run a small-area 1km UM on-demand). In 2009 a 1.5km UM was introduced into operations.

The next section discusses equation sets and approximations appropriate for NWP and climate modelling. This is followed by an outline of the ND scheme and then its coupling with physics. Section 5 describes the grids and UM configurations followed by a brief overview of idealised testing with ND in section 6. Section 7 is a recent history of ND followed by a few case study results to illustrate the advantage of the high resolution in forecasting severe weather events in section 8. This is followed by some of the issues raised by non-hydrostatic NWP and finally an outline of changes planned to address some of the weaknesses of the ND scheme.

2 Equations and approximations

The fully compressible (or non-hydrostatic) equations of motion are

$$\frac{D_{\underline{r}}u}{Dt} - \frac{uv}{\underline{r}}\tan\phi - 2\Omega\sin\phi v + \underline{\frac{uw}{r} + 2\Omega\cos\phi w} + \frac{1}{\rho\underline{r}\cos\phi}\frac{\partial p}{\partial\lambda} = F_u, \tag{1}$$

$$\frac{D_{\underline{r}}v}{Dt} + \frac{u^2}{\underline{r}}\tan\phi + 2\Omega\sin\phi u + \underline{\frac{vw}{r}} + \frac{1}{\rho\underline{r}}\frac{\partial p}{\partial\phi} = F_v, \tag{2}$$

$$\frac{D_{\underline{r}}w}{Dt} - \underline{\frac{u^2+v^2}{r} - 2\Omega\cos\phi u} + g + \frac{1}{\rho}\frac{\partial p}{\partial r} = F_w, \tag{3}$$

where

$$\frac{D_{\underline{r}}}{Dt} = \frac{\partial}{\partial t} + \frac{u}{\underline{r}\cos\phi}\frac{\partial}{\partial\lambda} + \frac{v}{\underline{r}}\frac{\partial}{\partial\phi} + w\frac{\partial}{\partial r},$$

and (F_u, F_v, F_w) are forcing terms e.g. from the parametrizations and/or diffusion.

The continuity equation is

$$\frac{D_{\underline{r}}\rho}{Dt} + \rho\nabla_{\underline{r}}.\mathbf{u} = 0, \tag{4}$$

where

$$\nabla_{\underline{r}}.\mathbf{u} = \frac{1}{\underline{r}\cos\phi}\left[\frac{\partial u}{\partial\lambda} + \frac{\partial(v\cos\phi)}{\partial\phi}\right] + \frac{1}{\underline{r}^2}\frac{\partial\left(\underline{r}^2 w\right)}{\partial r},$$

and the energy equation is

$$\frac{D_{\underline{r}}\theta}{Dt} = F_\theta, \tag{5}$$

with the equation of state

$$p = R\rho T. \tag{6}$$

These equations assume the Earth is spherical and that the surfaces of constant gravitational potential are spherical. This is referred to the spherical Earth approximation and effective gravity g is constant. These are the non-hydrostatic deep equations as used in the ND. The spherical Earth approximation in these equations should have g varying as $1/r^2$ (see White et al., 2005) for full consistency but the variation of g with height is small.

The quasi-hydrostatic approximation removes the $\frac{Dw}{Dt}$ term from equation (3). The shallow atmosphere approximation, where the depth of the atmosphere is assumed to be much smaller than the mean radius of the Earth a, replaces all the $\underline{r}$ in the equations above by the constant a together with the removal of the terms that are in red and underlined. These are additional metric terms and non-vertical (or $\cos\phi$) Coriolis terms which must be removed otherwise the shallow atmosphere equations do not satisfy conservation laws for energy or potential vorticity nor the axial angular momentum principle (White and Bromley, 1995). Perhaps it would be more appropriate to say (or at least to understand) the shallow atmosphere *and vertical Coriolis* approximation. The shallow atmosphere approximation is believed to be reasonable for large scales but at small scales, larger vertical velocities mean that the $\cos\phi$ Coriolis term in equation (1) probably cannot be safely neglected. The Coriolis terms neglected in the vertical momentum equation are generally much larger than the vertical acceleration so the shallow atmosphere approximation is unlikely to be appropriate for non-hydrostatic flows (see e.g. the scale analysis in Chapter 2 of Holton, 1992 and section 3 of White and Bromley, 1995).

The hydrostatic primitive equations make both the shallow atmosphere and hydrostatic approximations, so e.g. the horizontal momentum equations are:

$$\frac{Du}{Dt} - \frac{uv}{a}\tan\phi - 2\Omega\sin\phi v + + \frac{1}{\rho a\cos\phi}\frac{\partial p}{\partial\lambda} = F_u,$$

$$\frac{Dv}{Dt} + \frac{u^2}{a}\tan\phi + 2\Omega\sin\phi u + \frac{1}{\rho a}\frac{\partial p}{\partial\phi} = F_v,$$

where

$$\frac{D}{Dt} = \frac{\partial}{\partial t} + \frac{u}{a\cos\phi}\frac{\partial}{\partial\lambda} + \frac{v}{a}\frac{\partial}{\partial\phi} + w\frac{\partial}{\partial r}.$$

The scales for which the non-hydrostatic effects (or alternatively for which the hydrostatic approximation remains valid) is still a matter of debate. The prevailing view is that the hydrostatic approximation is valid in models with a resolution down to around 10km[1] and that below that non-hydrostatic effects become more important. However, the arguments involved are not precise enough to say exactly what is the appropriate resolution to drop the hydrostatic approximation (see e.g. Fig.3 in Daley, 1988 and his discussion therein) and it could be argued that 20km is advisable. Since between about 5 and 10km is often termed the grey zone due to the parametrization assumptions for deep convection becoming dubious and explicit convection inappropriate (see discussion in section 4) then 10km is convenient. However, at around a scale of 10km, the $\cos\phi$ Coriolis term in the vertical momentum equation (3) is comparable with the vertical acceleration for vertical velocities of $\sim$ 1m/s and is larger for smaller vertical velocities. Thus, there is a case for using the fully compressible equations even at 10km resolution. The only convincing proof of the suitability of using the fully compressible equations is to run a complete NWP system with a deep/shallow switch (both configurations and their data assimilation suitably tuned) and to compare forecast skill and systematic errors.

There are other approximations that can be made to the fully compressible equations to render them less compressible and therefore filter acoustic modes which might otherwise restrict the time step used in explicit time schemes. The normal modes of several approximations were examined by Davies et al. (2003) to establish their effects on the important meteorological modes of oscillation. The analysis was executed by including a set of switches which determines the nature of the approximation as indicated in table 1. The full details can be found in Davies et al. (2003) but the essential set of the switched linearised equations obtained are as follows:

$$\frac{Du}{Dt} + c_p\left(\bar\theta + \delta_E\theta'\right)\frac{\partial\pi'}{\partial x} - fv = 0$$

$$\frac{Dv}{Dt} + fu = 0,$$

$$\delta_V\frac{Dw}{Dt} + c_p\left(\bar\theta + \delta_E\theta'\right)\frac{\partial\pi'}{\partial z} + (1-\delta_B)c_p\frac{d\bar\theta}{dz}\pi' - \frac{g}{\bar\theta}\theta' = 0$$

$$\frac{\delta_A}{\bar\pi}\left\{\left(\frac{1-\kappa}{\kappa}\right)\frac{D}{Dt} + \frac{\partial u}{\partial x} + \frac{\partial w}{\partial z}\right\}\pi' + \frac{\partial u}{\partial x} + \left(\frac{\partial}{\partial z} + \frac{\delta_C}{\bar\rho}\frac{d\bar\rho}{dz} + \frac{\delta_D}{\bar\theta}\frac{d\bar\theta}{dz}\right)w = 0$$

The main conclusions from Davies et al. (2003) are:

[1] assuming that the minimum resolved scale is, say, between 50 to 100km

Equation set	Switches					
	δ_V	δ_A	δ_B	δ_C	δ_D	δ_E
Fully compressible	1	1	1	1	1	1
Hydrostatic	0	1	1	1	1	1
Pseudo-incompressible (Durran, 1989)	1	0	1	1	1	1
Anelastic (Wilhelmson and Ogura, 1972)	1	0	1	1	0	0
Anelastic (Lipps and Hemler, 1982)	1	0	0	1	0	0
Boussinesq	1	0	1	0	0	0

Table 1: Switch settings for equation sets

- Anelastic and Boussinesq equations are not suitable for NWP or climate modelling at any scale because they distort Rossby modes. They are suitable for process studies with shallow vertical scales.
- Pseudo-incompressible equations may be viable at small scales but not at large scales.
- Hydrostatic equations are good for large horizontal scales, although, unlike the fully compressible equations, the hydrostatic equations are not hyperbolic (Oliger and Sundström, 1978) .

The asymptotic properties of some of the above approximations are also examined in Cullen (2007) who also questions their suitability for NWP and climate modelling.

3 Overview of the UM New Dynamics scheme

3.1 New Dynamics design

The development of the ND for the UM aimed to improve accuracy by better treatment of the balanced part of the flow. Moreover, by eliminating or reducing the effect of computational modes (which lead to grid-splitting in the horizontal, Janjić, 1979) stability should improve without the need for excessive damping or diffusion. To include non-hydrostatic effects for future mesoscale modelling (and since the UM was already using the deep atmosphere equations) this meant using the fully compressible equations as described above. For large-scale modelling with the hydrostatic primitive equations, ECMWF had already demonstrated that semi-Lagrangian advection was much more efficient than Eulerian advection (Ritchie et al., 1995) but there were still issues to address when applying SISL schemes to the fully compressible equations (Golding, 1992). The various reasons for the overall design are mostly set out in Cullen et al. (1997) and Davies et al. (2005). A few additional remarks follow.

To optimize balance in the model and to eliminate computational modes, C-grid staggering in horizontal and Charney-Phillips staggering in the vertical were chosen. Whereas the advantages of C-grid staggering for the atmosphere are well-known (Arakawa and Lamb, 1981), its vertical counterpart, Charney-Phillips staggering presents a problem when used in boundary layer mixing as care is needed to define the mixing coefficients appropriately as momentum and temperature are at different levels. Arakawa and Konor (1996) showed that Charney-Phillips staggering avoided the computational mode present in Lorenz staggering (a result that was also demonstrated by Tony Hollingsworth in an unpublished note written as part of the development of the first ECMWF model). More recently Thuburn and Woollings (2005) compared several possible vertical staggerings and show that that used in the ND has the best properties.

The use of a semi-implicit time scheme and the construction of the elliptic equation for the pressure correction followed the work of Cullen (1989). Extending this to the fully-compressible equations and avoiding the use of a reference or basic state profile results in a 3-dimensional elliptic equation with variable coefficients for the pressure correction. This is solved iteratively using a restarted Generalised Conjugate Residual technique (Eisenstat et al., 1983,Smolarkiewicz et al., 2001) with appropriate pre-conditioning (Skamarock et al., 1997).

To apply conservation to tracers and non-negative quantities (monotonicity) under semi-Lagrangian advection, the Priestley (1993) algorithm is used. However, the algorithm cannot be used to conserve dry mass and it is only recently that conserving semi-Lagrangian schemes have become available (Zerroukat et al., 2002). In the ND an Eulerian treatment of the flux-form continuity equation for dry mass is used to achieve dry mass conservation.

3.2 New dynamics time-scheme

The governing equations are set out in Davies et al. (2005). The prognostic variables are the wind components (u,v,w), potential temperature θ, Exner pressure Π, dry density ρ_{dry} and mixing ratios of moist quantities defined as $m_X \equiv \rho_X/\rho_{dry}$ where X represents the various phases of water.

The governing equations can be written generically as

$$\frac{D\mathbf{X}}{Dt} = \mathbf{L}(\mathbf{x},t,\mathbf{X}) + \mathbf{N}(\mathbf{x},t,\mathbf{X}) + \mathbf{S}_1(\mathbf{x},t,\mathbf{X}) + \mathbf{S}_2(\mathbf{x},t,\mathbf{X}), \tag{7}$$

where

$$\frac{D}{Dt} \equiv \frac{\partial}{\partial t} + \mathbf{U}\cdot\nabla,$$

$\mathbf{X}$ is a vector of the prognostic variables, $\mathbf{x}$ denotes position, $\mathbf{L}$ represents dynamics terms linear in $\mathbf{X}$, $\mathbf{N}$ represents dynamics terms nonlinear in $\mathbf{X}$, $\mathbf{S}_1$ represents the "slow" physical source terms and $\mathbf{S}_2$ represents the "fast" physical source terms. In this scheme, only the convection and boundary layer (together with associated surface and cloud processes) are treated as "fast" processes; all other physical processes (radiation, gravity wave drag, large scale precipitation) are treated as "slow" processes. A target 2TL SISL discretization is given by

$$\frac{\mathbf{X}^{n+1} - \mathbf{X}^n_d}{\Delta t} = (1-\alpha)(\mathbf{L}+\mathbf{N}+\mathbf{S}_1+\mathbf{S}_2)^n_d + \alpha(\mathbf{L}+\mathbf{N}+\mathbf{S}_1+\mathbf{S}_2)^{n+1}. \tag{8}$$

The subscript d denotes evaluation at the departure point $\mathbf{x}_d$ and $\alpha \geq 1/2$ is the usual semi-implicit time-weighting coefficient. In practice, for an operational forecast model, it is computationally very expensive to solve this system of equations without making approximations to the terms at time-level $n+1$.

In the UM a predictor-corrector approach is used which is described schematically by the following steps:

$$\begin{aligned}
\mathbf{X}^{(1)} &= \mathbf{X}^n_d + (1-\alpha)\Delta t(\mathbf{L}+\mathbf{N})^n_d + \Delta t\,(\mathbf{S}_1)^n_d + \alpha\Delta t(\mathbf{L}+\mathbf{N})^n, && (9)\\
\mathbf{X}^{(2)} &= \mathbf{X}^{(1)} + \Delta t\mathbf{S}_2(\mathbf{X}^n, \mathbf{X}^{(1)}, \mathbf{X}^{(2)}), && (10)\\
\mathbf{X}^{(3)} - \alpha\Delta t\mathbf{L}^{(3)} &= \mathbf{X}^{(2)} + \alpha\Delta t(\mathbf{N}^* - \mathbf{N}^n - \mathbf{L}^n), && (11)
\end{aligned}$$

where $\mathbf{X}^{(1)}$ is the first predicted value, $\mathbf{X}^{(2)}$ is the predicted value after the "fast" physics processes and $\mathbf{X}^{(3)}$ the final predicted value. $\mathbf{L}^{(3)} \equiv \mathbf{L}(\mathbf{X}^{(3)})$ and $\mathbf{N}^*$ represents an estimate of the non-linear terms at t^{n+1} needed to make the system of equations tractable. $\mathbf{N}^*$ can contain contributions from any of the predictor states and the current state. The model state at time-level $n+1$ is $\mathbf{X}^{n+1} \equiv \mathbf{X}^{(3)}$, i.e. it is given by the final corrector. The "slow" physical processes are evaluated in parallel using data at time-level

n only (i.e. each process's tendency is independent of the other "slow" processes during a time-step). The "fast" physical processes are evaluated sequentially (i.e. the changes from all the other processes leading up to the "fast" physical processes are taken into account) and $\mathbf{S}_2(\mathbf{X}^n, \mathbf{X}^{(1)}, \mathbf{X}^{(2)})$ indicates the time-level of the input data used.

The discretization of the equations is described in Davies et al. (2005) and in Staniforth et al. (2006).

The off-centring parameters α, in the above equations, provide required damping to keep the scheme stable (see Staniforth et al., 2006) have different values for particular terms. $\alpha = 1$ for terms associated with acoustic modes and $\alpha = 0.7$ typically for the geostrophic balance terms. In most configurations there is no need to use any additional horizontal diffusion to run the ND since there is enough damping provided by the off-centring and the semi-Lagrangian interpolations. However, at high resolution where the vertical velocity is dominated by the diabatic forcing (see below) horizontal diffusion or turbulent mixing (Smagorinsky, 1963) is used to reduce small-scale noise.

Even though the horizontal grid is latitude-longitude (see section 5) filtering near the poles is not needed for stability. However, because of the use of an iterative solver, the anisotropy of the latitude-longitude grid results in a large number of solver iterations being required, particularly at high resolution. Alternating direction implicit (ADI) preconditioning (Skamarock et al., 1997) is insufficient (on its own) and it has been found that the use of a simple 1-2-1 filter applied multiply in the longitudinal direction near the poles further reduces the iterations with no apparent detriment.

4 Physics

Along with the change to the ND in the UM, the physics parametrizations were also changed (see Martin et al., 2006 for details). With the change of time scheme from split-explicit to semi-implicit the coupling with the physics also changed which provided an opportunity to make this coupling more optimal and achieve a better balance between the physics forcing and the dynamics. Physics coupling with 2TL SISL schemes was one of the topics discussed at a SRNWP workshops held at Météo France in December 1997 and in Prague in April 1999. Following the 1997 workshop, McDonald (1998) gave a presentation at the 1998 ECMWF seminars and later the physics-dynamics coupling in the IFS was modified (Wedi, 1999).

In a series of papers (Dubal et al., 2004, Dubal et al., 2005, Dubal et al., 2006) various physics-dynamics couplings were examined by requiring that the difference equations using large time steps should reproduce steady-states. The main conclusions were:

- Large time steps require vertical diffusion (boundary layer + convection) to be treated sequentially after all other processes (sequential splitting).
- Parallel-splitting needs small time steps.

In the ND time scheme, the slow processes (everything apart from the boundary layer mixing and convection) are treated in parallel at the start of the time step. The boundary layer mixing and convection are applied sequentially (i.e. taking into account all the other processes) after the semi-Lagrangian advection step but before the correction (solver) step.

In most models (probably all) the larger vertical velocities are a result of large-scale condensation and evaporation and as resolution increases maximum upward and downward vertical velocities tend to increase. The parametrization of convection at larger scales stabilizes the model atmosphere otherwise excessive large-scale condensation will occur (grid-point storms). The main motivation to run models at very high resolution is to allow convection to become organised but parametrized deep convection inhibits such organisation (and the parametrization assumptions become invalid). However, the resolution where some adjustment or mixing is required is probably much less that 1km and as resolution reduces (towards say 5km), explicit convection alone leads to excessive vertical velocities and rainfall (see Professor Arakawa's paper for this workshop). This should not be a surprise since resolved convection implies the minimum updraught and downdraught sizes to be the grid scale.

5 Grids and configurations

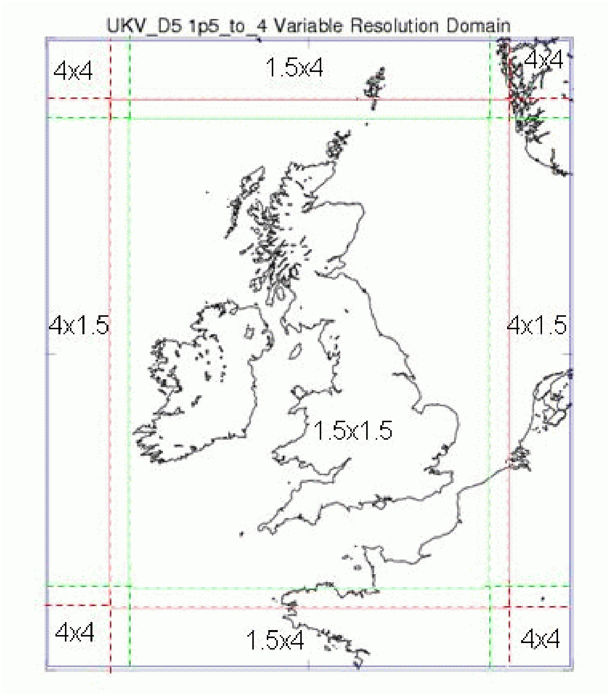

Figure 1: UKV domain and resolution in km. First and second values are East-West and North-South resolutions respectively. Most of the domain within the inner rectangle (green) has a resolution of 1.5x1.5km. Between the outer (red) rectangle and the domain boundary the resolution is 4km in the direction normal to the boundaries. Remaining regions have variable resolution where each grid-length inflates by about 10% towards the outer boundary.

The horizontal grid used for global configurations is regular latitude-longitude. For LAMs, the grid is usually rotated so that the grid Equator passes through the middle of the LAM thereby producing a near uniform resolution for domains that are not too large. Additionally for LAMs, the grid resolution can vary (Côté et al., 1998). This is done to minimize the scale difference between a LAM and driving model at and normal to the boundary as shown in Fig.1, which illustrates the grid used for the 1.5km UKV configuration. For processes that cannot be resolved by the lateral boundary data, using variable resolution reduces the mismatch of data at the boundaries which allows for a smoother transition between high resolution and the lateral boundary data. This allows small scale processes such as showers to develop before reaching the inner high resolution region. In addition to global configurations and LAMs that can be run anywhere, LAMs can be run bi-cyclic or cyclic East-West for idealised tests.

The vertical grid is height-based hybrid and terrain-following. The resolution is highest near the surface and stretches with height. The stretching is quadratic until upper-most levels where the stretching increases. Away from the surface ($\eta = 0$) the levels are gradually (quadratically) flattened until they become horizontal. It is desirable that the coordinate surfaces are horizontal as at as low an altitude as possible to minimize errors in the horizontal pressure gradient terms (Simmons and Burridge, 1981). To avoid introducing a discontinuity in $\partial r/\partial \eta$ at the first horizontal level altitude should be at least twice the height of the highest orography in the model domain.

6 Idealised testing

A range of idealised tests in various configurations (shallow water, 2-dimensional vertical slice and 3-dimensions) have been used as indicated in the list below. Some of these were executed during the initial design and development of the scheme and results are reported in Cullen et al. (1997) and Davies et al. (1998). Others have been (and continue to be used) to diagnose problems or evaluate formulation changes. The 3d flows over prescribed (simple) orography and dynamical core tests are available as options when running the UM as are options to run idealised test configurations for testing the physics parametrizations. The web page

$$http://box.mmm.ucar.edu/projects/srnwp\_tests/index.html$$

containing a set of standard tests for non-hydrostatic dynamical cores is maintained by the Mesoscale & Microscale Meteorology Division at NCAR.

- Shallow water test cases, Williamson et al. (1992)
- Idealised Eady-wave, Nakamura and Held (1989)
- A simulation of fog formation, Golding (1993)
- Vertically propagating sound waves, Golding (1992)
- Density currents, Straka et al. (1993)
- 2d and 3d flows over hills, e.g. Smith (1980), Pinty et al. (1995), Melvin et al. (2010)
- Steady flow over cosine hill.
- Convective bubble, Robert (1993)
- Dynamical core tests, Held and Suarez (1994)

7 Version histories and results

Development of a prototype ND in a full model with physics began in 1996. This was a stand-alone system with limited diagnostics compared with the UM. The first physics package used was from the HadCM3 climate model but in the later phase of development this was replaced by a new set of physics being developed for the UM climate model (Martin et al., 2006). Both global forecast and climate were developed in tandem. Global case studies using data either from the UM data or from ECMWF data were run at N216L30 (432*325, 60km, 40km top). These showed improvements to cross-polar flow (Fig.1 of Davies et al., 1998) and indicated a need for some polar filtering to reduce solver iterations. 3 year AMIP climate tests Gates et al. (1999) run at N48L38 (96*73) showed improved stratocumulus sheets west of California, Peru and South West Africa. In 2001, ND was built into UM system and coupled with 3DVAR for pre-operational (parallel) trials lasting nearly 1 year. During this period, various improvements and corrections were made and when the model forecast scores matched the operational UM the ND UM was made the operational global forecast model in 2002.

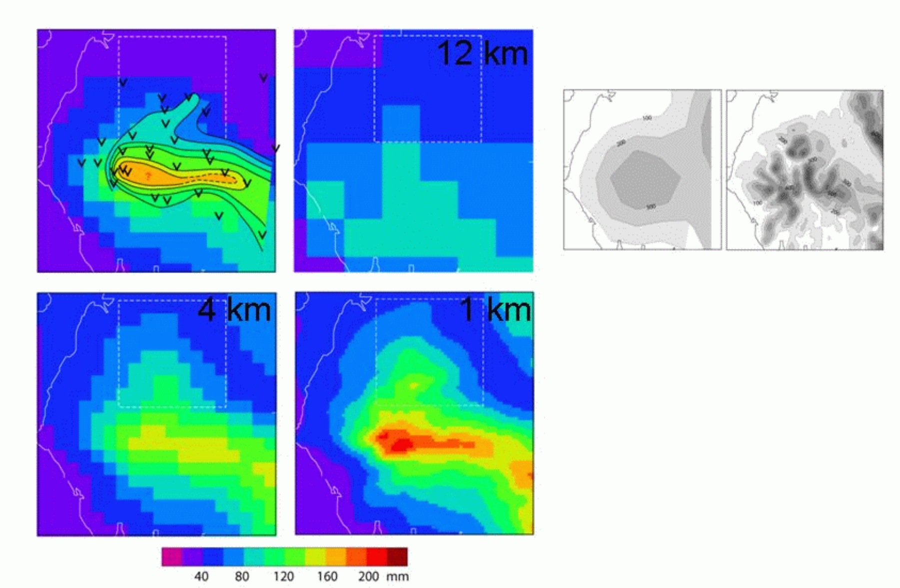

Figure 2: 24 hour rainfall accumulations for Carlisle floods of January 2005. Upper left shows analysed values using radar and rain gauges; Upper right panel shows the forecast accumulations from the 12km NAE; Lower panels show forecast accumulations from the UM run at 4km and 1km. The panels on the right show the model orography at 12km and 1km.

For LAM versions of ND the lateral boundary scheme is well-posed (Oliger and Sundström, 1978). The well-posedness is achieved by being non-hydrostatic (the hydrostatic equations are not well-posed due to the diagnostic equation for the vertical velocity) and by using an upwinding (SL) scheme. There is also a need to apply lateral boundary conditions (lbcs) in the Helmholtz equation and to use blending (Davies, 1976) to account for mis-matching of data which may occur from data differences between the lbcs and the LAM.

The notable events and a brief history of ND are listed below. The N designation refers to the number of intervals in the longitudinal half-circumference, i.e. 2N intervals around a latitude circle. L is the number of vertical levels. Typically, the latitudinal resolution is chosen so that the grid-boxes are almost square in mid-latitudes, i.e. approximately 1.5N intervals from pole to pole.

- Global model N216L38, 432*325, operational in August 2002 on the CRAY t3e.
- UK Mesoscale model 15km operational in October 2002,
- North Atlantic and European (NAE) 15km LAM replaced UK Mesoscale model, December 2002.
- NEC SX6/8 Spring 2004. 4DVAR October 2004.
- HadGEM1 (N96L38) spin-up run started May 2004.
- NAE resolution increased to 12km February 2005.
- Global N320L50, 640*481, 40km 63km top, December 2005.
- UK LAM at 4km resolution (UK4), 288*360, 38 levels quasi-operational April 2005 (after Boscastle storm, August 2004).
- UK4, 4km 70 levels, 40km top, November 2007.

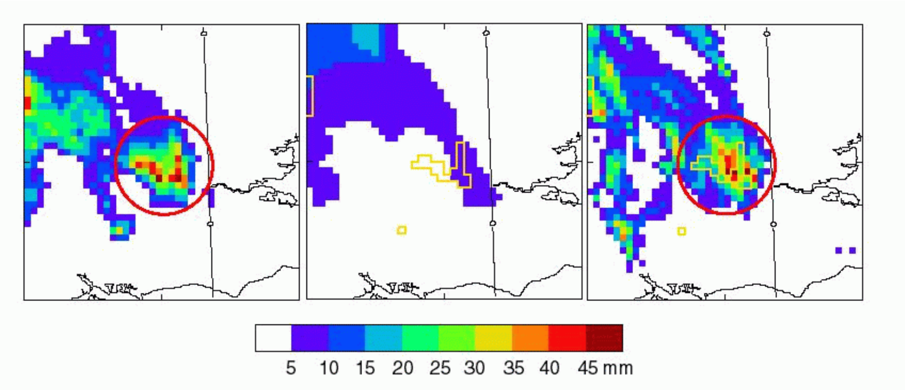

Figure 3: Flooding in London on 3rd August 2004. 5 hour rainfall accumulations from radar (left panel), UM forecast from T+4 to T+9 at 12km (middle panel) 1km (right panel).

- HiGEM (N144L38), NuGEM (N216L38), HadGEM3(N96L85)
- IBM Power 6 spring 2009.
- UKV, 744*928, 1.5km, variable resolution to 4km around edges, see Fig. 1, operational summer 2009.
- Global 70 levels 80km top, November 2009.
- Global N512L70, 1024*769, 25km February 2010.

Results from routine verification show that the skill of the global UM forecast system has continued (and continues) to improve since the ND became operational. Much of the improvement of forecast skill is due to improvements in data assimilation (of which the model is a component) and through better use and availability of more observations from satellites. However, during that time there have also been enhancements to the resolution in both the horizontal and vertical and improvements to the physics. The dynamics has hardly changed since it became operational. Most dynamics changes have been associated with resolution and optimization.

The climate configurations of the UM, HadGEM contains aerosols and dust, a carbon cycle and is coupled with an ocean and ice models. Climate configurations with higher horizontal resolution have also been developed (HiGEM, 288*217, Shaffrey et al., 2009 and, on the Earth Simulator in Japan, NuGEM, 432*325). The climate configurations are currently being evaluated with increased vertical resolution and with lids at around 80km.

8 High resolution case studies

The UK LAM at 4km resolution (UK4) was introduced operationally in 2007 to provide local NWP forecasts. This followed several years of case study work and its use in the Convective Storms Initiation Project (CSIP) observational campaign, Browning et al. (2007). In recent years there have been several notable precipitation events in the UK which have afforded opportunities to evaluate the UM at scales where non-hydrostatic effects are important. Some cases were run using a 1km LAM covering part of the UK and test versions of the UKV which is mostly 1.5km resolution but varying to 4km around domain edges, see Fig. 1. A few examples are presented here to illustrate the performance of ND at high resolutions.

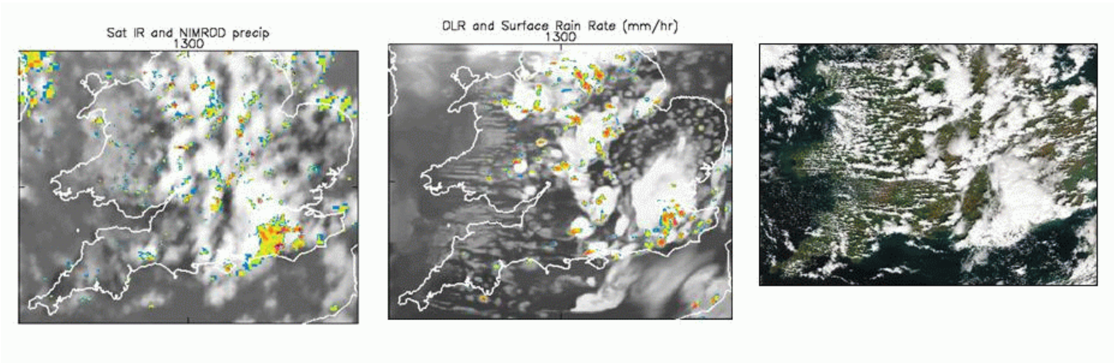

Figure 4: A showery day, 25th August 2005. Left panel, satellite IR image and radar rainfall rates; middle panel, 10 hour forecast from UKV; right panel, visible image from MODIS satellite.

8.1 Carlisle case

Fig. 2 shows 24 hour rainfall accumulations for the Carlisle floods of January 2005. The upper left panel shows analysed values using radar data and rain gauges. The upper right panel shows the forecast accumulations from the 12km NAE whilst the lower panels show forecast accumulations from the UM run at 4km and 1km. The two small panels on the right show the model orography at 12km and 1km resolution. The extra detail associated with increased detail in the orography is typical of events where frontal rain persists for several hours or more.

8.2 London case

Fig. 3 shows 5 hour rainfall accumulations between 11 and 16 UTC on 3rd August 2004 for SE England. The left panel shows data from radar and the next two panels show model accumulations between T+4 and T+9 at 12km and 1km. More than 80mm of rain was measured in parts of northwest London which led to flash flooding and major disruption to traffic. The 1km UM was able to produce realistic rainfall totals for London and from studying rainfall rates (not shown) indicated some regeneration of new convective cells on the south-eastern part of the main band. However, some other details of the rainfall elsewhere do not match the radar.

8.3 Showery day

The final example is not from a particularly noteworthy event but from a (breezy?) showery summer day in August 2005. Fig. 4 shows a composite IR image and radar rainfall rates on the left and a visible image on the right. The centre panel is a 10 hour forecast of rainfall rate and the outgoing long-wave radiation (OLR) from the 1.5km UKV. Although individual showers do not match, the larger scale features of the rainfall and cloud are well-captured, including the streaks in the cloud over Wales and the South West.

9 Issues with high resolution modelling

The case studies above demonstrate the effectiveness of higher resolution for capturing features at smaller scales, especially those details related to the the surface forcing. However, smaller scale features have short predictability timescales and quantities which such high spatial variability (e.g. heavy rain and fog) may be predictable for only a few hours at most. This means that for these quantities, direct model output is not a sensible way of extracting the forecast signal. Instead, if forecast information is aggregated (in space and time) more reliable forecast information can be obtained (Roberts and Lean, 2008).

As discussed in section 4, there is a tendency for excessive precipitation and vertical velocities at the grid-scales (grid-point storms) which probably indicates the need for some additional mixing (in the horizontal as well as vertical) and/or some adjustment in the vertical.

At present it is not known whether explicit convection reduces systematic errors and/or improves variability at larger scales (e.g. the Madden-Julian oscillation, ENSO, etc.) since running globally long enough and at high enough resolution is not yet possible at the Met Office.

In the high resolution modelling at the Met Office, no obvious problems have been encountered with semi-Lagrangian advection with relatively large (by comparison with explicit schemes) time steps and hence Courant numbers. In nearly all meteorological problems the trajectories for the strongest winds are well-represented by straight lines (a standard assumption for semi-Lagrangian trajectories) even with large time steps. In flows with significant curvature then the straight line trajectories may cross unless the time step is reduced (so that the flow Courant number is much less than unity) thereby eliminating the advantage of semi-Lagrangian advection. In idealised tests where such effects might be important (e.g. Straka et al., 1993 density current, convective bubbles Robert, 1993) they are due to turbulence so direct numerical simulation is not necessary. In numerical simulation of intense thunderstorms it is likely that large time steps could not be maintained but so far in high resolution studies with the ND other factors such as lack of mixing appear to be the primary concern.

10 Future UM development: ENDGame

The predictor-corrector scheme would have been iterated if acceptable results could not have been achieved with just one application of the scheme. For a more typical SISL scheme, scheme where a reference state is used and the equations are separated in the vertical, then it appears that such a scheme needs to be iterated, see e.g. Bénard (2003). Iteration does not appear to be necessary for 2TL SISL schemes applied to the hydrostatic equations provided the reference state is chosen carefully (Simmons and Temperton, 1997). However, even for the hydrostatic equations, stability is improved with iteration since in the first iteration the advecting winds are extrapolated in time to obtain time-level $n+\frac{1}{2}$ values whereas subsequent iterations can use advecting winds interpolated in time by using the new estimates winds at time-level $n+1$. Iterative time-stepping is an option in the ND and tests on sets of case studies demonstrated an increase in skill achieved at lower cost than increasing resolution (Diamantakis et al., 2007). However, at a fixed resolution, iterating the time-step increases the cost of the model by around 60% as both the dynamics and "fast" physics are repeated.

The ND scheme has some deficiencies the removal of which may improve its performance and increase its robustness. These are:

1. The Eulerian treatment of density needed to conserve mass renders the scheme unstable unless there is some off centring of the time scheme which results in slightly reduced accuracy in some idealised tests.
2. The use of a non-interpolating scheme in the vertical for potential temperature θ.
3. Explicit treatment of the non-vertical Coriolis terms.
4. Scalars at the poles.

It is proposed to address these weaknesses as follows:

- To conserve mass (and tracers) use SLICE (Semi-Lagrangian Inherently Conserving and Efficient, Zerroukat et al., 2002, Zerroukat et al., 2009, Zerroukat et al., 2009, Melvin et al., 2010).
- Remove individual off-centring, extract reference profile and use iterative time-stepping.
- Fully-interpolating tri-cubic Lagrange or spline scheme for potential temperature θ.
- Non-vertical Coriolis terms treated implicitly to improve Rossby mode dispersion.
- v-at-the-poles (Thuburn and Staniforth, 2004).

These changes are the ENDGame (Even Newer Dynamics for General Atmospheric Modelling of the Environment) project for the UM. The scheme is currently being tested and full model testing with UM physics is expected to begin in 2011.

As previously noted in section 2, g should vary with height in the deep equations (White et al., 2005) even for the spherical Earth approximation. Furthermore, ENDGame can use the fully compressible equations without the spherical Earth approximation. An option to employ a spheroidal coordinate system (White et al., 2008) will allow gravity to vary with height and latitude more accurately although whether this is worthwhile will need to be evaluated. Switches in the code will permit ENDGame to use spherical coordinates or a Cartesian system. Switches will also be used to compare deep/shallow atmosphere and the hydrostatic approximation with the fully compressible equations.

As with many models using implicit time stepping, the non-locality of the solver may become an issue on massively parallel (10^5 or more processors) computers. Any non-local process such as fast Fourier transforms or 1-2-1 filters may limit the speed of the model, as will data transposes. In the longer term, more uniform grids (on the sphere) may be necessary but most have some degree of grid-imprinting which will require thorough investigation, especially for climate modelling. In the short term the Yin-Yang grid (Li et al., 2008) may be an option for ENDGame but discussion of alternative options is beyond the scope of this paper.

Acknowledgments

Many Met Office scientists and former colleagues (and several participants at this workshop) have made significant contributions to the work reported in this paper. I particularly acknowledge the help and advice (and congeniality) of Mike Cullen, Andrew Staniforth, Andy White and Nigel Wood. Thanks to Peter Clark, Humphrey Lean and Nigel Roberts for supplying the figures and associated background information.

References

Arakawa, A. and C. S. Konor (1996). Vertical differencing of the primitive equations based on the Charney-Phillips grid in hybrid σ-p vertical coordinates. *Mon. Wea. Rev. 124*, 511–528.

Arakawa, A. and V. R. Lamb (1981). A potential enstrophy and energy conserving scheme for the shallow-water equations. *Mon. Wea. Rev. 109*, 18–36.

Ballard, S. P., B. W. Golding, and R. N. B. Smith (1991). Mesoscale Model Experimantal Forecasts of the Haar of Northeast Scotland. *Mon. Wea. Rev. 119*, 2107–2123.

Bénard, P. (2003). Stability of semi-implicit and iterative centered-implicit time discretizations for various equation systems used in NWP. *Mon. Wea. Rev. 131*, 2479–2491.

Browning, K. A., C. J. Morcrette, J. Nicol, A. M. Blyth, B. J. B. L. J. Bennett and, J. Marsham, S. D. Mobbs, D. J. Parker, F. Perry, P. A. Clark, S. P. Ballard, M. A. Dixon, R. M. Forbes, H. W. Lean, Z. Li, N. M. Roberts, U. Corsmeier, C. Barthlott, B. Deny, N. Kalthoff, S. Khodayar, M. Kohler, C. Kottmeier, S. Kraut, M. Kunz, J. Lenfant, A. Wieser, J. L. Agnew, D. Bamber, J. McGregor, K. M. Beswick, M. D. Gray, E. Norton, H. M. A. Ricketts, A. Russell, G. Vaughan, A. R. Webb, M. Bitter, T. Feuerle, R. Hankers, H. Schulz, K. E. Bozier, C. G. Collier, F. Davies, C. Gaffard, T. J. Hewison, D. N. Ladd, E. C. Slack, J. Waight, M. Ramatschi, D. P. Wareing, and R. J. Watson (2007). The convective storm initiation project. *Bull. Amer. Meteor. Soc. 88*, 1939–1955.

Carpenter, K. M. (1979). An experimental forecast using a non-hydrostatic mesoscale model. *Q. J. R. Meteorol. Soc. 105*, 629–655.

Côté, J., J.-G. Desmarais, S. Gravel, A. Méthot, A. Patoine, M. Roch, and A. Staniforth (1998). The operational CMC-MRB Global Environmental Multiscale (GEM) model. Part II: Mesoscale results. *Mon. Wea. Rev. 126*, 1373–1395.

Cullen, M. (2007). Modelling atmospheric flows. *Acta Numerica*, 1–87.

Cullen, M. J. P. (1989). Implicit finite-difference method for modelling discontinuous atmospheric flows. *J. Comp. Phys. 81*, 319–348.

Cullen, M. J. P. and T. Davies (1991). A conservative split-explicit integration scheme with fourth-order horizontal advection. *Q. J. R. Meteorol. Soc. 117*, 993–1002.

Cullen, M. J. P., T. Davies, M. H. Mawson, J. A. James, S. C. Coulter, and A. Malcolm (1997). An overview of numerical methods for the next generation UK NWP and climate model. In C. Lin, R. Laprise, and H. Ritchie (Eds.), *Numerical Methods in Atmospheric Modelling, The André Robert memorial volume*, Ottawa, Canada, pp. 425–444. Canadian Meteorological and Oceanographical Society.

Daley, R. (1988). The normal modes of the spherical non-hydrostatic equations with applications to the filtering of acoustic modes. *Tellus 40A*, 96–106.

Davies, H. C. (1976). A lateral boundary formulation for multi-level prediction models. *Q. J. R. Meteorol. Soc. 102*, 405–418.

Davies, T., M. Cullen, A. Malcolm, M. Mawson, A. Staniforth, A. White, and N. Wood (2005). A new dynamical core for the Met Office's global and regional modelling of the atmosphere. *Q. J. R. Meteorol. Soc. 131*, 1759–1782.

Davies, T., M. J. P. Cullen, M. H. Mawson, and A. J. Malcolm (1998). A new dynamical formulation for the UK Meteorological Office Unified Model. In *ECMWF Seminar Proceedings: Recent Developments in Numerical Methods for Atmospheric Modelling*, Reading, pp. 202–225. ECMWF.

Davies, T., A. Staniforth, N. Wood, and J. Thuburn (2003). Validity of anelastic and other equation sets as inferred from normal-mode analysis. *Q. J. R. Meteorol. Soc. 129*, 2761–2775.

Diamantakis, M., T. Davies, and N. Wood (2007). An iterative time-stepping scheme for the Met Office's semi-implicit semi-Lagrangian non-hydrostatic model. *Q. J. R. Meteorol. Soc. 133*, 997–1011.

Dubal, M., N. Wood, and A. Staniforth (2004). Analysis of parallel versus sequential splittings for time-stepping physical parameterizations. *Mon. Wea. Rev. 132*, 121–132.

Dubal, M., N. Wood, and A. Staniforth (2005). Mixed parallel-sequential split schemes for time-stepping multiple physical parameterisations. *Mon. Wea. Rev. 133*, 989–1002.

Dubal, M., N. Wood, and A. Staniforth (2006). Some numerical properties of approaches to physics-dynamics coupling for NWP. *Q. J. R. Meteorol. Soc. 132*, 27–42.

Durran, D. R. (1989). Improving the anelastic approximation. *J. Atmos. Sci. 46*, 1453–1461.

Eisenstat, S. C., H. C. Elman, and M. H. Schultz (1983). Variational iterative methods for nonsymmetric systems of linear equations. *SIAM J. Numer. Anal. 20*, 345–357.

Gadd, A. J. (1978). A split-explicit scheme for numerical weather prediction. *Q. J. R. Meteorol. Soc. 104*, 569–582.

Gates, W. L., J. S. Boyle, C. Covey, C. G. Dease, C. M. Doutriaux, R. S. Drach, M. Fiorino, P. J. Gleckler, J. J. Hnilo, S. M. Marlais, T. J. Phillips, G. L. Potter, B. D. Santer, K. R. Sperber, K. E. Taylor, and D. N. Williams (1999). An overview of the results of the atmospheric model intercomparison project (AMIP I). *Bull. Amer. Meteor. Soc. 80*, 29–56.

Golding, B. W. (1987). The U.K. Meteorological Office Mesoscale Model. *Bound. Layer Meteor. 41*, 97–107.

Golding, B. W. (1992). An efficient non-hydrostatic forecast model. *Meteorol. Atmos. Phys. 50*, 89–103.

Golding, B. W. (1993). A Study of the Influence of Terrain on Fog Development. *Mon. Wea. Rev. 121*, 2529–2541.

Held, I. M. and M. J. Suarez (1994). A proposal for the intercomparison of dynamical cores of atmospheric general circulation models. *Bull. Amer. Meteor. Soc. 75*, 1825–1830.

Holton, J. R. (1992). *An introduction to dynamic meteorology* (3rd ed.). New York: Academic Press.

Janjić, Z. I. (1979). The forward-backward scheme modified to prevent two-grid-interval noise and its application in σ coordinate models. *Contrib. Atmos. Phys. 52*, 69–84.

Li, X., D. Chen, X. Peng, K. Takahashi, and F. Xiao (2008). A Multimoment Finite-Volume Shallow-Water Model on the Yin-Yang Overset Spherical Grid. *Mon. Wea. Rev. 136*, 3066–3086.

Lipps, F. B. and R. S. Hemler (1982). A scale analysis of deep moist convection and some related numerical calculations. *J. Atmos. Sci. 39*, 2192–2210.

Martin, G. M., M. A. Ringer, V. D. Pope, A. Jones, C. Dearden, and T. J. Hinton (2006). The physical properties of the atmosphere in the new Hadley Centre Global Environment Model, HadGEM1. Part i: Model description and global climatology. *J. Climate 19*, 1274–1301.

McDonald, A. (1998). The origin of noise in semi-Lagrangian integrations. In *ECMWF Seminar Proceedings: Recent Developments in Numerical Methods for Atmospheric Modelling*, Reading, pp. 308–334. ECMWF.

McDonald, A. and J. R. Bates (1987). Improving the estimate of the departure point in a two-time level semi-Lagrangian and semi-implicit scheme. *Mon. Wea. Rev. 115*, 737–739.

Melvin, T., M. Dubal, N. Wood, A. Staniforth, and M. Zerroukat (2010). An inherently mass-conserving iterative semi-implicit semi-Lagrangian discretization of the non-hydrostatic vertical-slice equations. *Q. J. R. Meteorol. Soc. 136*, 799–814.

Nakamura, N. and I. M. Held (1989). Nonlinear equilibration of two-dimensional Eady-waves. *J. Atmos. Sci. 46*, 3055–3064.

Oliger, J. and A. Sundström (1978). Theoretical and practical aspects of some initial boundary value problems in fluid dynamics. *SIAM J. Appl. Math. 35*, 419–446.

Pinty, J.-P., R. Benoit, E. Richard, and R. Laprise (1995). Simple tests of a semi-implicit semi-Lagrangian model on 2d mountain wave problems. *Mon. Wea. Rev. 123*, 3042–3058.

Priestley, A. (1993). A quasi-conservative version of the semi-Lagrangian advection scheme. *Mon. Wea. Rev. 121*, 621–629.

Ritchie, H., C. Temperton, A. Simmons, M. Hortal, T. Davies, D. Dent, and M. Hamrud (1995). Implementation of the semi-Lagrangian method in a high resolution version of the ECMWF forecast model. *Mon. Wea. Rev. 123*, 489–514.

Robert, A. (1993). Bubble convection experiments with a semi-implicit formulation of the Euler equations. *J. Atmos. Sci. 50*, 1865–1873.

Roberts, N. M. and H. W. Lean (2008). Scale-Selective Verification of Rainfall Accumulations from High-Resolution Forecasts of Convective Events. *Mon. Wea. Rev. 136*, 78–97.

Shaffrey, L. C., I. Stevens, W. A. Norton, M. J. Roberts, P. L. Vidale, J. D. Harle, A. Jrrar, D. P. Stevens, M. J. Woodage, M. E. Demory, J. Donners, D. B. Clark, A. Clayton, J. W. Cole, S. S. Wilson, W. M. Connolley, T. Davies, A. M. Iwi, T. C. Johns, J. C. King, A. L. New, J. M. Slingo, A. Slingo, L. Steenman-Clark, and G. M. Martin (2009). U.K. HiGEM: The New U.K. High-Resolution Global Environment Model - Model Description and Basic Evaluation. *J. Climate 22*, 1861–1896.

Simmons, A. J. and D. M. Burridge (1981). An energy and angular-momentum conserving vertical finite-difference scheme and hybrid vertical coordinates. *Mon. Wea. Rev. 109*, 758–766.

Simmons, A. J. and C. Temperton (1997). Stability of a two-time-level semi-implicit integration scheme for gravity wave motion. *Mon. Wea. Rev. 125*, 600–615.

Skamarock, W. C., P. K. Smolarkiewicz, and J. B. Klemp (1997). Preconditioned conjugate-residual solvers for Helmholtz equations in nonhydrostatic models. *Mon. Wea. Rev. 125*, 587–599.

Smagorinsky, J. (1963). General Circulation Experiments with the Primitive Equations. *Mon. Wea. Rev. 91*, 99–164.

Smith, R. B. (1980). Linear theory of stratified hydrostatic flow past an isolated mountain. *Tellus 32*, 348–364.

Smolarkiewicz, P. K., L. G. Margolin, and A. A. Wyszogrodzki (2001). A class of nonhydrostatic global models. *J. Atmos. Sci. 58*, 349–364.

Staniforth, A. and J. Côté (1991). Semi-Lagrangian integration schemes for atmospheric models - a review. *Mon. Wea. Rev. 119*, 2206–2223.

Staniforth, A., A. White, N. Wood, J. Thuburn, M. Zerroukat, E. Cordero, and T. Davies (2006). The Joy of U.M. 6.3 − model formulation, Unified Model Documentation Paper No. 15. Available online at http://www.metoffice.com/research/nwp/publications/papers/unified_model/index.html.

Straka, J. M., R. B. Wilhelmson, L. J. Wicker, J. R. Anderson, and K. K. Drogemeier (1993). Numerical solutions of a non-linear density current: A benchmark solution and comparisons. *Int. J. Num. Meth. Fluids 17*, 1–22.

Tapp, M. C. and P. W. White (1976). A non-hydrostatic mesoscale model. *Q. J. R. Meteorol. Soc. 102*, 277–295.

Temperton, C. and A. Staniforth (1987). An efficient two-time-level semi-Lagrangian semi-implicit integration scheme. *Q. J. R. Meteorol. Soc. 113*, 1025–1039.

Thuburn, J. and A. Staniforth (2004). Conservation and linear Rossby-mode dispersion on the spherical C grid. *Mon. Wea. Rev. 132*, 641–653.

Thuburn, J. and T. J. Woollings (2005). Vertical discretizations for compressible Euler equation atmospheric models giving optimal representation of normal modes. *J. Comput. Phys. 203*, 386–404.

Wedi, N. P. (1999). The numerical coupling of the physical parametrizations to the "dynamical" equations in a forecast model. ECMWF Technical Memorandum No. 274, pp. 37.

White, A. A. and R. A. Bromley (1995). Dynamically consistent, quasi-hydrostatic equations for global models with a complete representation of the Coriolis force. *Q. J. R. Meteorol. Soc. 121*, 399–418.

White, A. A., B. J. Hoskins, I. Roulstone, and A. Staniforth (2005). Consistent approximate models of the global atmosphere: shallow, deep, hydrostatic, quasi-hydrostatic and non-hydrostatic. *Q. J. R. Meteorol. Soc. 131*, 2081–2107.

White, A. A., A. Staniforth, and N. Wood (2008). Spheroidal coordinate systems for modelling global atmospheres. *Q. J. R. Meteorol. Soc. 134*, 261–270.

Wilhelmson, R. and Y. Ogura (1972). The pressure perturbation and the numerical modeling of a cloud. *J. Atmos. Sci. 29*, 1295–1307.

Williamson, D. L., J. B. Drake, J. J. Hack, R. Jakob, and P. N. Swarztrauber (1992). A standard test set for numerical approximations to the shallow-water equations in spherical geometry. *J. Comp. Phys. 102*, 211–224.

Zerroukat, M., N. Wood, and A. Staniforth (2002). SLICE: A Semi-Lagrangian Inherently Conserving and Efficient scheme for transport problems. *Q. J. R. Meteorol. Soc. 128*, 2801–2820.

Zerroukat, M., N. Wood, and A. Staniforth (2009). An improved version of SLICE for conservative monotonic remapping on a C-grid. *Q. J. R. Meteorol. Soc. 135*, 541–546.

Zerroukat, M., N. Wood, A. Staniforth, A. White, and J. Thuburn (2009). An inherently mass-conserving semi-implicit semi-Lagrangian discretisation of the shallow water equations on the sphere. *Q. J. R. Meteorol. Soc. 135*, 1104–1116.